

# The symmetric broadening of the water relaxation peak in polymer–water mixtures and its relationship to the hydrophilic and hydrophobic properties of polymers

Yaroslav E. Ryabov<sup>a)</sup> and Yuri Feldman<sup>b)</sup>

*Department of Applied Physics, The Hebrew University of Jerusalem, Givat Ram, 91904, Jerusalem, Israel*

Naoki Shinyashiki and Shin Yagihara

*Department of Physics, Tokai University, Hiratsuka-shi, Kanagawa 259-1292, Japan*

(Received 5 September 2001; accepted 27 February 2002)

The dielectric relaxation of water molecules in polymer–water mixtures is discussed. The memory function approach and scaling relationships are used as a basis for the model of symmetric dielectric spectrum broadening. The correspondence between the relaxation time, the geometrical properties, the self-diffusion coefficient, and the Cole–Cole exponent is established. The relationship between the hydrophilic and hydrophobic properties of the polymers and the dielectric relaxation parameters is discussed. © 2002 American Institute of Physics. [DOI: 10.1063/1.1471551]

## I. INTRODUCTION

An extensive study of water and its interaction with the interface has attracted much attention recently. Substantial progress has been made in unraveling the inherent complexities of water–substrate interactions, with most of the attention focused on water in biopolymers, synthetic polymers, and amphiphilic systems.<sup>1</sup> It is now well known that the physical properties of water molecules near surfaces (be they inorganic or organic, as in surfactant-based systems) differ measurably from those of bulk water molecules. This observation underlies the distinction between “bound” and “free” water. The principal dielectric relaxation peak of water exhibits the Debye-type relaxation curve<sup>2–7</sup> in spite of the complexities of hydrogen-bonding liquids on the molecular level. The relaxation curve of water has been considered to be due to the hydrogen-bonding network structure constructed by water molecules behaving as large clusters.<sup>8–10</sup> The relaxation of the large clusters occurs via the Brownian diffusion process, i.e., this process requires many individual steps of molecular reorientation. Furthermore, water shows another relaxation process at a frequency of about one order of magnitude higher than that of the principal relaxation<sup>4–7</sup> frequency. This relaxation process was thought to be caused by the flipping motion of free OH groups between two acceptor sites and/or the breaking and reforming of a given hydrogen bond in a translational motion.<sup>4–11</sup>

For water in mixtures of organic materials, the shape of the relaxation curve of the water depends on the molecular size of the solute.<sup>12–20</sup> The primary dielectric relaxation of water in mixtures with small organic compounds exhibits a broad and asymmetric relaxation curve.<sup>12–17</sup> This relaxation behavior can be interpreted from the cooperative motion of water and solute molecules.<sup>15,16</sup> On the other hand, the relax-

ation process of water in the water mixture of a random-coiled polymer shows a symmetric relaxation curve.<sup>16–20</sup> The relaxation time and width of the dielectric spectrum increases with increasing polymer concentration. In the polymer–water mixture, the polymer chain is too large to move cooperatively with water molecules. The polymer chain behaves as a geometric constraint for rotational motion of water molecules and their movement is strongly hindered by the polymer chain. The variations of conformations of random-coiled polymer induce variation in the local structure of water, which yields the symmetric relaxation curve.<sup>15,16,18</sup>

In order to discuss the relationship between the polymer structure and the dynamical feature of the water in the polymer–water mixture, dielectric relaxations of water for seven kinds of polymer–water mixtures were observed.<sup>18</sup> All the relaxation curves show the symmetric relaxation described by the Cole–Cole equation.<sup>21</sup> The symmetrical broadening of the dielectric spectrum was phenomenologically interpreted by the variation of the local structure of water.<sup>18</sup> Plots of the relaxation times against the parameters for the symmetrical broadening of the relaxation curve can be classified into two groups of polymer structures: hydrophobic polymers and hydrophilic ones. The hydrophobic polymer group contained nonelectrolyte polymers and the hydrophilic polymer group mainly contained electrolyte polymers. The relaxation curve for the latter group is broader than that of the former, when compared at the same relaxation time. This result was interpreted to indicate that the water structure in the mixtures of the hydrophobic polymer was uniform and stable than that in the mixtures of the hydrophilic polymers. In this paper, we will present the model that explains the experimental observation mentioned above<sup>18</sup> and which establishes that the relationship between the relaxation time, the geometrical properties, the self-diffusion coefficient, and the Cole–Cole exponent of the water relaxation peaks in polymer–water mixtures.

<sup>a)</sup>Permanent address: Institute for Mechanics and Engineering of Kazan Scientific Center of RAS, Lobochevsky st. 2/31, P.O. Box 559, 420111, Kazan, Russia.

<sup>b)</sup>Electronic mail: yurif@vms.huji.ac.il

## II. EXPERIMENTAL PROCEDURE

The polymers investigated in this work were poly(vinylpyrrolidone) (PVP; average molecular weight  $M_w = 10\,000$ ), poly(ethylene glycol) (PEG;  $M_w = 8000$ ), poly(ethylene imine) (PEI;  $M_w = 500\,000$ ), poly(acrylic acid) (PAA;  $M_w = 5000$ ), poly(vinyl methyl ether) (PVME;  $M_w = 90\,000$ ), poly(allylamine) (PAA;  $M_w = 10\,000$ ), and poly(vinyl alcohol) (PVA;  $M_w = 77\,000$ ). Water used in this experiment was distilled and deionized by milli-Q (MILLIPORE Co., Ltd.). Water mixtures of these polymers were prepared in the concentration range from 10 wt % to 20–85 wt % of polymer. Dielectric measurements of the polymer–water mixtures were performed in a frequency range from 300 MHz to 10 GHz at 25 °C, employing the method of time domain reflectometry (TDR). The sample preparations<sup>18</sup> and the procedures for the dielectric measurement<sup>22,23</sup> have already been reported.

## III. THE MODEL

The complex dielectric permittivity  $\varepsilon^*(\omega)$  for the Cole–Cole process is represented in the frequency domain as

$$\varepsilon^*(i\omega) = \varepsilon_\infty + \frac{\varepsilon_s - \varepsilon_\infty}{1 + (i\omega\tau)^\alpha}, \quad (1)$$

where  $\omega$  is the cyclic frequency,  $i$  is the imaginary unit,  $0 < \alpha \leq 1$  is the phenomenological so-called Cole–Cole exponent,  $\varepsilon_\infty$  is the high-frequency limit of the complex dielectric permittivity  $\varepsilon^*(\omega)$ ,  $\varepsilon_s$  is the static dielectric permittivity, and  $\tau$  is the relaxation time.<sup>21</sup> The specific case of Eq. (1) with  $\alpha = 1$  is correspondent to Debye’s relaxation, while  $0 < \alpha < 1$  represents the symmetric broadening of the relaxation peak.

One of several arguments that can explain the non-Debye relaxation is the memory effect.<sup>24–31</sup> In this case, the normalized dipole correlation function  $f(t)$  corresponding to a nonexponential dielectric relaxation process obeys the equation

$$\frac{df(t)}{dt} = - \int_0^t m(t-t')f(t')dt', \quad (2)$$

where  $m(t)$  is the memory function and  $t$  is the time variable. In the case of dielectric relaxation,  $f(t)$  can be considered as a dipole correlation function. The specific form of the memory function is dependent on the characteristics of interaction between the relaxing system and the statistical reservoir.<sup>30,31</sup>

In the frequency domain, after a Laplace transform<sup>32</sup> Eq. (2) reads as

$$zF(z) - 1 = -M(z)F(z), \quad (3)$$

where  $z$  is the Laplace parameter,  $F(z)$  and  $M(z)$  are Laplace images of  $f(t)$  and  $m(t)$ . Thus, after some simple algebra combining (1) with (3) and taking into account the relationship between the complex permittivity and the correlation function,<sup>33</sup>  $[\varepsilon^*(z) - \varepsilon_\infty]/(\varepsilon_s - \varepsilon_\infty) = 1 - zF(z)$ , one can obtain the Laplace image of the memory function for the Cole–Cole process as follows:

$$M(z) = z^{1-\alpha}\tau^{-\alpha}. \quad (4)$$

The mathematical implication is that  $M(z)$  in (4) is a multi-sheet function<sup>32</sup> of complex variable  $z$ . In order to represent this function in time domain one should select the schlicht domain using supplementary reasons. These computational constraints can be avoided by using Riemann–Liouville fractional differential operator.<sup>34,35</sup> By defining the fractional differentiation operator  ${}_0D_t^{1-\alpha}$ , we have  ${}_0D_t^{1-\alpha}[f(t)] := z^{1-\alpha}F(z) - C$ , where  $C = {}_0D_t^{-\alpha}[f(t)]|_{t=+0}$  is a constant which is dependent on the initial condition,  ${}_0D_t^{-\nu}[g(t)] = [\Gamma(\nu)]^{-1} \int_0^t (t-t')^{\nu-1} g(t') dt'$  is the Riemann–Liouville fractional integration operator ( $0 < \nu \leq 1$ ),  ${}_0D_t^\gamma[g(t)] = (d/dt)D_0^{\gamma-1}[g(t)]$  is the Riemann–Liouville fractional derivation operator ( $0 < \gamma \leq 1$ ), “:=” denotes the Laplace transformation, and  $\Gamma(\nu)$  is the gamma function. Thus, Eq. (3) with the memory function (4) in time domain can be rewritten as follows:

$$\frac{df(t)}{dt} = -\tau^{-\alpha} {}_0D_t^{1-\alpha}[f(t)] + C. \quad (5)$$

Note that the constant  $C$  can be easily obtained from this equation. In fact, the relationship between the complex susceptibility and the correlation function, together with Eq. (1) and (5), leads directly to the requirement that  $C = 0$ .

This equation was already discussed<sup>24–27,36</sup> as a phenomenological representation of the dynamic equation for the Cole–Cole law. The convolution of fractional deferential operator in Eq. (5) shows that this equation can be regarded as consequence of the memory effect. A comprehensive discussion of the memory function (4) properties was already presented.<sup>24–26</sup> Accordingly, Eq. (5) holds for some cooperative domain and describes the relaxation of an ensemble of microscopic units. Each unit has its own microscopic memory function  $m_\delta(t)$ , which describes the interaction between this unit and the surroundings (interaction with the statistical reservoir). The main idea of such an interaction suggests<sup>24–26</sup> that  $m_\delta(t) \sim \sum_i \delta(t_i - t)$  [see Fig. 1(a)]. It reflects the interrupted interaction between the relaxing unit and its neighbors. The time moments  $t_i$  (the time position of the delta functions) are the moments of the interaction (relaxation acts). The works<sup>24–26</sup> imply that the sequence of  $t_i$  constructs a fractal set (the Cantor set for example) with a fractal dimension  $0 < d_f \leq 1$ . This statement is related to the idea that cooperative behavior provides some ordering and long-lasting scaling of relaxation process. Following these assumptions, the memory function  $m(t)$  for a cooperative domain can be obtained as a result of averaging over the ensemble of  $m_\delta(t)$  [see Fig. 1(b), where for more convenient representation  $I(t) = \int_0^t m(t') dt'$  is plotted instead of  $m(t)$ ]. The requirements of measure conservation<sup>24,26</sup> in the interval  $[0, 1/\xi]$  and conservation of the fractal dimension  $d_f$  for all  $m_\delta(t)$  give this averaging as

$$m(t) = \int_{-1/2}^{1/2} m_\delta(\xi^{-u}t) \xi^{-u(1-d_f)} du,$$

and

$$M(z) \sim z^{1-d_f}. \quad (6)$$

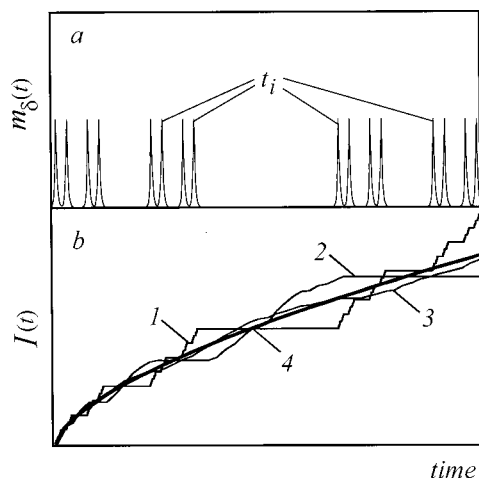


FIG. 1. (a) Schematic picture of  $m_\delta(t)$  dependency.  $t_i$  are the time moments of the interaction in time that construct a fractal Cantor set with the dimension  $d_f = \ln 2 / \ln 3 \approx 0.63$ . (b) Schematic representation that illustrates the averaging of  $m(t)$  over an ensemble of microscopic units. Here,  $I(t) = \int_0^t m(t') dt'$ . Curve 1 corresponds to the cooperative ensemble of a single microscopic unit with  $t_i$  distributed by the Cantor set. Curve 2 represents the ensemble of 3 units of the same type. Curve 3—ten units. The curve 4 corresponds to the 1000 units in ensemble. The last one displays the power-law behavior  $I(t) \sim t^{\ln 2 / \ln 3}$ .

These requirements are direct consequences of the idea that all microscopic units are equivalent. In general, not only the fractal structure of events, but other physical reasons can determine the power-law time dependence of the macroscopic memory function (6). For example, the model<sup>37</sup> describes the scaling of dynamic coefficients (microelastic stiffens and viscosity) that leads to the power-law asymptotic frequency dependency of complex modulus in polymers.

According to the averaging procedure (6) the memory function (4) is a cooperative one and the Cole–Cole behavior appears on the macroscopic level after averaging over the ensemble of microscopic dipole active units. Comparing (4) and (6), one can establish that  $\alpha = d_f$ . This result once again highlights the fact that in this model the fractal properties on a microscopic level can induce the power-law behavior of memory functions (4) and Cole–Cole permittivity (1) on a macroscopic level.

By definition,<sup>38</sup> the fractal dimension is given by

$$d_f = \alpha = \frac{\ln(N)}{\ln(\xi)}. \quad (7)$$

Here, the scaling parameter  $\xi$  is the dimensionless time interval size and  $N$  is the number of delta functions (relaxation acts) in the interval. However, a characteristic time constant of the Cole–Cole process is the relaxation time  $\tau$ . Thereby, the scaling parameter  $\xi$  and the relaxation time should be proportional to each other

$$\xi = \frac{\tau}{\tau_0}, \quad (8)$$

where the constant minimal  $\tau_0$  is the cutoff time of the scaling in time.

There is a computer simulation proof<sup>39</sup> that an anomalous relaxation on a fractal structure exhibits a Cole–Cole

behavior. Hence, in this work we will assume that the memory function (6) has its origin in the geometrical self-similarity of the polymer network. Thus, the scaling parameter  $N$  actually is the number of points where the relaxing units are interacting with the statistical reservoir (i.e., by the ergodic assumption—the number of relaxation acts on a microscopic level for a cooperative domain). The assumption of geometrical self-similarity of the considered system suggests that this number is

$$N = G \left( \frac{R}{R_0} \right)^{d_G}, \quad (9)$$

where  $d_G$  is a spatial fractal dimension of the point set where relaxing units are interacting with the surroundings.  $R$  is the size of a sample volume section where movement of one relaxing unit occurs.  $R_0$  is the cutoff size of the scaling in the space or the size of the cooperative domain.  $G$  is a geometrical coefficient about unity, which depends on the shape of the system heterogeneity. For instance, the well-known two-dimensional recursive fractal Sierpinski carpet<sup>38</sup> has  $d_G = \ln(8)/\ln(3) \approx 1.89$ ,  $G = \sqrt{3}/4 \approx 0.43$ .

In general, the dielectric relaxation can be regarded as rotation of macroscopic dielectric polarization vector of some representative sample volume. It is clear that this rotation is provided by some microscopic motions including mobility and transport of individual charge carriers. In the simplest case, these microscopic processes can be related to rotation of independent microscopic dipoles. In general, however, such an idea does not explain correctly the mechanism of dielectric relaxation. For example, hopping transport of charge carriers, dielectric relaxation in polymers or in associated liquids cannot be reduced to the problem of independent microscopic dipole rotation.

The main goal of this research is the study of water relaxation in polymer–water mixture. The dispersion of bulk water is observed in microwave frequency range<sup>1,2</sup> ( $\sim 2 \cdot 10^{10}$  Hz) that is much higher than the relaxation of macromolecules in aqueous solution ( $10^5$ – $10^8$  Hz) by itself. For example, the relaxation of local part of macromolecule observed in the frequency range between 100 kHz–100 MHz for the water mixtures<sup>23</sup> of PVP and PVME. Therefore, in our case we assume that the polymer chains are immobile in the frequency interval studied.

The water molecules interact with each other through the hydrogen bonds network. For this reason dielectric relaxation of bulk water is cooperative and cannot be derived from independent microscopic dipoles concept. In this regard, the tetrahedral displacement model<sup>40</sup> of water molecule dynamics should be mentioned. The model takes into account the relaxation of macroscopic dipole moment provided by reorientation of water molecules and their diffusion simultaneously, considering only the collective behavior of water molecules. In our model we will discuss the single water molecule behavior and imply that each reorientation of a water molecule is accompanied by its jump to the other position. In other words, the relaxation of a water molecule is accompanied by an act of diffusion. Thereby, the macroscopic relaxation time is the time during which the relaxing

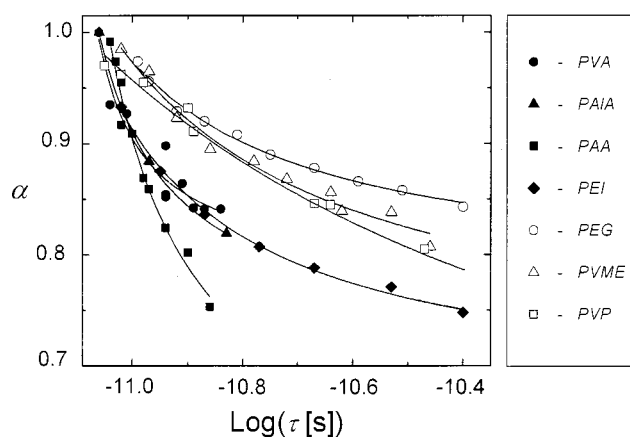


FIG. 2. Cole–Cole exponent  $\alpha$  vs relaxation time  $\tau$ . The curves are fitted to Eq. (11). The full symbols correspond to the mixtures of hydrophilic polymers and water while the open symbols correspond to the mixtures of hydrophobic polymers and water.

microscopic unit would move some distance  $R$ . The Einstein–Smoluchowski theory<sup>41,42</sup> gives the relationship between  $\tau$  and  $R$  as follows:

$$R^2 = 2d_E D_s \tau, \quad (10)$$

where  $D_s$  is the self-diffusion coefficient, and  $d_E$  is the Euclidean dimension. Thus, by substitution of (8), (9), and (10) into (7), one can get the relationship between the Cole–Cole parameter  $\alpha$  and the relaxation time  $\tau$  in the form

$$\alpha = \frac{d_G \ln(\tau \omega_s)}{2 \ln(\tau/\tau_0)}, \quad (11)$$

where  $\omega_s = 2d_E G^{2/d_G} D_s / R_0^2$  is the characteristic frequency of the self-diffusion process.

#### IV. RESULTS AND DISCUSSION

The experimental dependencies of the Cole–Cole exponent  $\alpha$  versus relaxation time  $\tau$ , together with fitting curves according to Eq. (11) with three fitting parameters  $d_G$ ,  $\tau_0$ , and  $\omega_s$  for all the samples, are plotted in Fig. 2. As mentioned above, Fig. 2 shows a remarkable separation of the experimental curves into two groups. The hydrophilic polymer solutions PVA, PAIA, PAA, and PEI are distributed in one group while the hydrophobic polymer water mixtures PEG, PVME, and PVP are in another. Note that the curves of the hydrophobic group are above those of the hydrophilic group.

According to the presented model the Cole–Cole exponent reflects the interaction between the relaxing units and the statistical reservoir. The biggest deviation of the Cole–Cole exponent from unity corresponds to the strongest interaction. We can consider that in our case the relaxing units are the water molecules, while the statistical reservoir is the polymer macromolecule. The deviation  $\alpha$  from unity for the hydrophilic group (see Fig. 2) is greater than that of the hydrophobic one. This indicates that the water–polymer interaction is more significant for the hydrophilic samples and thus confirms the concept presented here.

Figure 2 also shows that for all samples the experimental curves rise up to  $\alpha=1$  at  $\tau \sim 8$  ps. This point corresponds to 0% of polymer in water and to the relaxation of bulk water. Increasing the polymer concentration leads to the increase of the relaxation time and to the decrease of the Cole–Cole exponent. At the same time, the change of the Cole–Cole exponent is an integral effect. When discussing the interaction between the relaxation units and the statistical reservoir, we are assuming that this interaction includes within itself the interactions of the water molecules with each other in the cooperative domain, the confinement and caging of the water molecules by the polymer chains, as well as other types of interactions. Caging and confinement in particular depend on the local structure, and for this reason the scaling properties become central in the consideration.

In the framework of the presented model  $R$  is the size of the water molecules' cooperative region affected by the polymer chains. The structure of the water molecules in this dynamic cooperative domain is different from the cooperative structure of the bulk water. The size of this cooperative region grows with the increase of the polymer concentration. The increase of the polymer concentration results in the growth of the cooperative area size  $R$ , which consequently leads to the increase of the relaxation time  $\tau$ . The cooperativity implies a long-range space correlation; therefore, at nonzero polymer concentrations all the water molecules (at least all of the water molecules which contribute to the discussed relaxation process) are within the cooperative region, whose structure is different from the structure of bulk water.

It is well known<sup>2,3</sup> that the macroscopic dielectric relaxation time of the bulk water (8.27 ps at 25 °C) is about ten times greater than the microscopic relaxation time of a single water molecule, which is about one hydrogen bond lifetime<sup>4–7</sup> ( $\sim 0.7$  ps). This fact follows from the associative structure of bulk water, where the macroscopic relaxation time reflects the cooperative relaxation process related to the space scale of the cooperative region.

As mentioned above, the water in the polymer–water mixture is organized into specific cooperative structures that are different from that of the bulk water. This microscopic relaxation of water molecules in that pattern depends on the dynamic properties of the cooperativity and rate of interaction with a polymer matrix. Different polymers perturb the bulk water structure in different ways and activate specific cooperative water domains with different microscopic relaxation times.

In the framework of our model the microscopic relaxation time of the water molecule is equal to the cutoff time of the scaling in time domain  $\tau_0$ . For the most hydrophilic polymer PVA, the strong interaction between the polymer and the water molecule results in the greatest value of microscopic relaxation time  $\tau_0$ , which is only 10% less than the macroscopic relaxation time of the bulk water (see Table I). Weakening of the hydrophilic properties (or intensification of the hydrophobic properties) results in a decrease of interaction between the water and the polymer and consequently in a decrease of  $\tau_0$ . The aqueous solution of the most hydrophobic polymer PVP has the smallest value of a single water molecule microscopic relaxation time, which is

TABLE I. Values of the space fractional dimension  $d_G$ , the cutoff time of scaling in the time domain  $\tau_0$ , the characteristic frequency  $\omega_s$  and the estimated self-diffusion coefficient for the sample.

Sample	$d_G$	$\tau_0$ [ps]	$\omega_s \times 10^{-11}$ [Hz]	$D_s \times 10^9$ [m <sup>2</sup> s <sup>-1</sup> ]
PVA	1.56 ± 0.09	7.18 ± 0.74	1.47 ± 0.21	3.31
PAIA <sup>a</sup>	1.43	6.46	1.74	3.92
PAA	1.12 ± 0.17	6.34 ± 0.83	2.08 ± 0.68	4.68
PEI	1.33 ± 0.02	4.89 ± 0.45	2.67 ± 0.40	6.01
PEG	1.54 ± 0.04	4.45 ± 0.74	2.78 ± 0.63	6.26
PVME	1.38 ± 0.10	3.58 ± 1.23	4.24 ± 2.47	9.54
PVP	1.00 ± 0.01	0.79 ± 0.11	127 ± 34	286

<sup>a</sup>For the sample PAIA there are only three experimental points. For this reason it is impossible to determine the mean square deviation value and consequently the confidence intervals for the fitting parameters.

almost equal to the microscopic relaxation time of bulk water (see Table I).

The interaction between the water and the polymer matrix actually occurs in the vicinity of the polymer chains, and only the water molecules located in this interface are affected by the interaction. The space fractal dimension  $d_G$  in this case is the dimension of the interface. This quantity is not a direct measure of the polymer chain structure but corresponds to some specific length scale pertinent to the relaxation process. The generally acknowledged models<sup>43</sup> point to large-scale dimensions of the polymer chains, either 2 (in ideal case of a concentrated solution) or 5/3 (in a dilute solution in a good solvent). Nevertheless, one could recognize that the fitted values of  $d_G$ , presented in Table I, fall into the interval  $1 < d_G < 2$  and are in good agreement with the values mentioned above. In this regard one could consider the value of  $d_G$  as a measure of polymer structure at the intermediate scale. Remarkably, according to the data obtained by fitting, the weakening of the hydrophilic property leads to a decrease in  $d_G$  and probably to the straightening of the polymer chains (see Table I).

The presence of a polymer in water affects both relaxation and diffusion of the solvent. To estimate the self-diffusion coefficient, we can use the following expression:

$$D_s \cong \frac{\omega_s R_0^2}{2d_E}, \quad (12)$$

which directly follows from the definition of the characteristic frequency of the self-diffusion process  $\omega_s$ . It is assumed in the last expression that the geometrical factor is  $G = 1$ . In our case the scaling cutoff size in the space is equal to the size of a water molecule,  $R_0 \approx 3 \text{ \AA}$ . The Euclidean dimension of the space where the diffusion occurs is the nearest integer number greater than the fractal dimension. Thus,  $d_E = 2$ . The results of the estimation are presented in Table I. Note that the polymer affects only water molecules situated in the vicinity of the polymer chains. This means that the estimated self-diffusion coefficient corresponds only to these water molecules and is not dependent on the polymer concentration. The averaged self-diffusion coefficient estimated for the whole polymer–water mixture should be different and depend on the polymer concentration. This coefficient does not characterize the mixture as a whole but reflects only the water–polymer interaction.

The self-diffusion coefficient for the bulk water<sup>44</sup> at 25 °C is  $2.57 \times 10^{-9} \text{ m}^2 \text{ s}^{-1}$ . The presence of a polymer in the water prevents the bulk water structure formation and promotes the diffusion. However, the strong interaction between polymer and water for hydrophilic samples inhibits the diffusion. From Table I we can see the clear tendency of the diffusion coefficient to increase with a decrease of hydrophilicity. For the most hydrophilic sample PVA the estimated self-diffusion coefficient is only 30% greater than for the bulk water, while for the PVP sample it is about two orders of magnitude higher (see Table I).

## V. CONCLUSION

The main dielectric relaxation peak for bulk water is due to the cooperative relaxation on the scale of the water molecule cluster. Thus, the presence of macromolecules in aqueous solutions changes the water structure and water–water interactions. The changes depend on the concentration of the impurities as well as on the features of interaction between the water and the macromolecules.

The model was elaborated to establish the relationship between the relaxation time, the geometrical properties (space fractal dimension  $d_G$ ), the self-diffusion coefficient, and the Cole–Cole exponent. It was shown that the microscopic relaxation time of water molecules in the vicinity of the polymer matrix correlates with the hydrophilicity of the impurities. At the same time, it was observed that the increase of hydrophobicity of the impurities increases the diffusion of the water molecules in the cooperative domains near the polymer chains.

- <sup>1</sup>F. Frank, in *Water, A Comprehensive Treatise*, edited by F. Frank (Plenum, New York, 1975), Vol. 4.
- <sup>2</sup>J. B. Hasted, in *Water, A Comprehensive Treatise*, edited by F. Frank (Plenum, New York, 1972), Vol. 1, Chap. 7, p. 255.
- <sup>3</sup>U. Kaatze, *J. Chem. Eng. Data* **34**, 371 (1989).
- <sup>4</sup>J. Barthel, K. Bachhuber, R. Buchner, and H. Hetzenauer, *Chem. Phys. Lett.* **165**, 369 (1990).
- <sup>5</sup>U. Kaatze, *J. Mol. Liq.* **56**, 95 (1993).
- <sup>6</sup>R. Buchner, J. Barthel, and J. Stauber, *Chem. Phys. Lett.* **306**, 57 (1999).
- <sup>7</sup>C. Ronne, P. Astrad, and S. R. Keiding, *Phys. Rev. Lett.* **82**, 2888 (1999).
- <sup>8</sup>C. A. Angell, in *Hydrogen-bonded Liquids*, edited by J. C. Dore and J. Teixeira (Kluwer Academic, The Netherlands, 1991), p. 59.
- <sup>9</sup>J. Crossely and G. Williams, *J. Chem. Soc., Faraday Trans. 2* **73**, 1906 (1977).
- <sup>10</sup>M. A. Floriano and C. A. Angell, *J. Chem. Phys.* **91**, 2537 (1989).
- <sup>11</sup>O. Conde and J. Teixeira, *J. Phys. (Paris)* **44**, 525 (1983).
- <sup>12</sup>S. Mashimo, T. Umehara, and H. Redlin, *J. Chem. Phys.* **95**, 6257 (1991).
- <sup>13</sup>F. Wang, R. Pottel, and U. Kaatze, *J. Phys. Chem. B* **101**, 922 (1997).
- <sup>14</sup>S. Sudo, Y. Kitsuki, N. Shinyashiki, and S. Yagihara, *J. Phys. Chem. A* **106**, 458 (2002).
- <sup>15</sup>N. Shinyashiki, S. Sudo, W. Abe, and S. Yagihara, *J. Chem. Phys.* **109**, 9843 (1998).
- <sup>16</sup>N. Shinyashiki and S. Yagihara, *J. Phys. Chem. B* **103**, 4481 (1999).
- <sup>17</sup>U. Kaatze, *Adv. Mol. Relax. Processes* **7**, 71 (1975).
- <sup>18</sup>N. Shinyashiki, I. Arita, S. Yagihara, and S. Mashimo, *J. Phys. Chem. B* **102**, 3249 (1998).
- <sup>19</sup>N. Shinyashiki, N. Asaka, S. Mashimo, and S. Yagihara, *J. Chem. Phys.* **93**, 760 (1998).
- <sup>20</sup>U. Kaatze, O. Gottman, R. Podbielski, R. Pottel, and U. Terveer, *J. Phys. Chem.* **82**, 112 (1978).
- <sup>21</sup>K. S. Cole and R. H. Cole, *J. Chem. Phys.* **9**, 341 (1941).
- <sup>22</sup>S. Mashimo and N. Miura, *J. Chem. Phys.* **99**, 9874 (1993).

- <sup>23</sup>N. Miura, N. Shinyashiki, and S. Mashimo, *J. Chem. Phys.* **97**, 8722 (1992).
- <sup>24</sup>A. Le Mehaute, R. Nigmatullin, and L. Nivanen, *Fleches du Temps et Geometry fractale* (Hermez, Paris, 1998)
- <sup>25</sup>R. R. Nigmatullin and Ya. E. Ryabov, *Phys. Solid State* **39**, 87 (1997).
- <sup>26</sup>Ya. E. Ryabov, Ph.D. thesis, Kazan State University (1996).
- <sup>27</sup>*Applications of Fractional Calculus in Physics*, edited by R. Hilfer (World Scientific, London, 2000).
- <sup>28</sup>R. Metzler and J. Klafter, *Phys. Rep.* **339**, 1 (2000).
- <sup>29</sup>I. M. Sokolov, *Phys. Rev. E* **63**, 011104 (2001).
- <sup>30</sup>H. Mori, *Prog. Theor. Phys.* **33**, 423 (1965).
- <sup>31</sup>H. Mori, *Prog. Theor. Phys.* **34**, 399 (1965).
- <sup>32</sup>J. A. Korn and T. M. Korn, *Mathematical Handbook* (McGraw-Hill, New York, 1968).
- <sup>33</sup>C. J. F. Bottcher and P. Bordewijk, *Theory of Electric Polarization* (Elsevier, Amsterdam, 1992).
- <sup>34</sup>K. Oldham and J. Spanier, *The Fractional Calculus* (Academic, New York, 1974).
- <sup>35</sup>K. Miller and B. Ross, *An Introduction to the Fractional Calculus and Fractional Differential Equations* (Wiley, New York, 1993).
- <sup>36</sup>K. Weron and A. Klauzer, *Ferroelectrics* **236**, 59 (2000).
- <sup>37</sup>H. Schiessel and A. Blumen, *Fractals* **3**, 483 (1995).
- <sup>38</sup>J. Feder, *Fractals* (Plenum, New York, 1988).
- <sup>39</sup>S. Fujiwara and F. Yonezawa, *Phys. Rev. E* **51**, 2277 (1995).
- <sup>40</sup>N. Agmon, *J. Chem. Phys.* **100**, 1072 (1996).
- <sup>41</sup>A. Einstein, *Ann. Phys. (Leipzig)* **322**, 549 (1905).
- <sup>42</sup>P. K. Pathria, *Statistical Mechanics* (Pergamon, Oxford, 1972).
- <sup>43</sup>A. Yu. Grosberg, A. R. Khokhlov, *Statistical Physics of Macromolecules* (Nauka, Moscow, 1989; English translation: American Institute of Physics, New York, 1994).
- <sup>44</sup>D. Eisenberg and W. Kauzmann, *The Structure and Properties of Water* (Clarendon, Oxford, 1969).